Interdiffusion and exchange coupling in Cr overlayers on a Fe(001) substrate

I. Turek,[1,2] M. Freyss,[3,4] P. Weinberger,[2] D. Stoeffler,[4] and H. Dreyssé[4]
[1]*Institute of Physics of Materials, Academy of Sciences of the Czech Republic, Žižkova 22, CZ-61662 Brno, Czech Republic*
[2]*Center for Computational Materials Science, Technical University of Vienna, Getreidemarkt 9/158, A-1060 Vienna, Austria*
[3]*Institut für Festkörperforschung, Forschungszentrum Jülich, D-52425 Jülich, Germany*
[4]*Institut de Physique et de Chimie des Matériaux de Strasbourg, 23, rue du Loess, F-67037 Strasbourg Cedex, France*
(Received 26 June 2000; published 18 December 2000)

The influence of interfacial interdiffusion on the magnetic order in ultrathin epitaxial Cr films on a Fe(001) substrate was studied by means of electronic structure calculations. The total coverage of the films was assumed to be one, two, and six monolayers of Cr while the interdiffusion was simulated by two-dimensional Cr-Fe alloys in the two atomic layers forming the Cr/Fe interface. Two limiting cases were considered: (i) perfectly ordered alloys, described in terms of a semiempirical tight-binding method using the recursion technique, and (ii) substitutionally disordered alloys, whose electronic structure was determined *ab initio* using the tight-binding linear muffin-tin orbital method and the coherent-potential approximation. In both cases, the magnetic coupling of the Cr overlayer to the ferromagnetic Fe substrate exhibits similar transitions (π phase shifts) due to varying compositions at the interface. The calculated results provide additional support for recent interpretations of experiments on Fe/Cr/Fe(001) trilayers.

DOI: 10.1103/PhysRevB.63.024413 PACS number(s): 75.70.Ak, 75.70.Cn

I. INTRODUCTION

The discovery of the oscillatory interlayer coupling in Fe/Cr(001) multilayers a decade ago[1,2] initiated extensive research of this layered system. At present, a general agreement exists regarding the two types of oscillations of exchange coupling in Fe/Cr/Fe(001) trilayers: the short period of about two monolayers (ML) is related directly to the antiferromagnetic ground state of bulk bcc Cr, whereas the longer period (12 ML) can be explained by the Cr Fermi surface.[3] However, the experimentally observed phase of the short period[4,5] is opposite to that predicted theoretically.[3,6] A similar situation was reported for epitaxial Cr thin films on a Fe(001) substrate:[4] in contrast to theoretical expectations, the measured magnetization of the top surface Cr layer is antiparallel (parallel) to the Fe magnetization for an even (odd) number of Cr layers.

A possible explanation of this discrepancy was suggested on the basis of electronic structure calculations[7] and has been verified by recent experiments on Fe-whisker/Cr/Fe(001) systems:[5] the reversal of exchange coupling is due to interdiffusion at the Cr/Fe interface, which is often found in this system under the usual preparation conditions.[5,8–10] However, the validity of the conclusions in Ref. 7 should be accepted with caution for two reasons: (i) the interdiffusion was simulated using two-dimensional-ordered Cr-Fe alloys formed in one or two monolayers at the interface, and (ii) the electronic structure of the model systems was calculated using a semiempirical tight-binding (SE-TB) *d*-band Hamiltonian.

Similarly, recent first-principles calculations of spin structures in Fe/Cr superlattices with intermixing considered only ordered alloys at the interface.[11,12] The main purpose of the present work is to perform a study complementary to Refs. 7,11 and 12, namely, to simulate the interdiffusion in terms of random (substitutionally disordered) two-dimensional (2D) alloys and to determine the corresponding electronic and magnetic structure within the local spin-density approximation (LSDA) and the coherent-potential approximation (CPA). For the sake of completeness, we present the previous SE-TB results[7] together with the new LSDA-CPA ones. Finally, we compare both sets of obtained data and relate them to other theoretical and experimental findings.

II. MODELS

We considered epitaxial Cr overlayers on a Fe(001) substrate with all atoms occupying the positions of an ideal bcc lattice (parent lattice) with the experimental lattice constant of pure iron. The interdiffusion at the Cr/Fe interface was simulated by the following composition in the atomic layers:

$$\mathrm{vac}/\mathrm{Cr}_n/\mathrm{Cr}_{1-x}\mathrm{Fe}_x/\mathrm{Cr}_x\mathrm{Fe}_{1-x}/\mathrm{Fe}(001), \tag{1}$$

where x is a concentration variable ($0 \leqslant x \leqslant 1$) and n denotes the number of pure Cr layers. This model refers to a chromium film of a total coverage $(n+1)$ ML Cr with interdiffusion confined to a two-monolayer region, which approximates quite well the chemical profiles in experimental samples.[5] The limit of $x=0$ corresponds to the case without interdiffusion, while the opposite limit of $x=1$ describes a complete exchange of one monolayer of Fe and Cr at the interface. We performed the study for $n=0$, 1, and 5, which is equivalent to 1, 2, and 6 ML Cr/Fe(001), respectively. We considered ordered 2D alloys as well as substitutionally disordered (random) 2D alloys. In the case of the ordered alloys studied here and in Ref. 7, the 2D unit cells employed are shown in Fig. 1; they correspond to the following discrete set of the concentration variable x:

$$x = 0.11,\ 0.25,\ 0.33,\ 0.5,\ 0.67,\ 0.75,\ 0.89, \tag{2}$$

while, in the case of the random alloys, the concentration range was sampled by

$$x = 0,\ 0.1,\ 0.3,\ 0.5,\ 0.7,\ 0.9,\ 1, \tag{3}$$

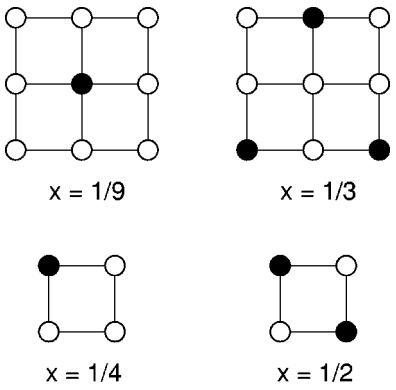

FIG. 1. Unit cells of the ordered alloys for special values of concentration x. In here, Cr atoms are shown as empty circles and Fe atoms as full circles. The unit cells for the complementary concentration ($x'=1-x$) are obtained by an exchange of the atomic species.

where the limits $x=0$ and $x=1$ describe perfect layers, in which single impurities can be considered.

III. COMPUTATIONAL TECHNIQUES

The electronic structure and the local magnetic moments for the systems with ordered interfacial alloys were calculated by means of the SE-TB method and the recursion technique. The models with random alloys were treated by an *ab initio* approach based on the tight-binding linear muffin-tin orbital (TB-LMTO) method and the CPA. In both cases, only collinear magnetic structures were assumed.

A. Semiempirical tight-binding method

In the SE–TB method, the electronic wave function is expanded in a fixed basis of atomic orbitals. Here, only the atomic d orbitals $|im\sigma\rangle$ are taken into account, where i labels the atomic sites, m refers to the type of d orbital, and σ is the spin index ($\sigma=+,-$). The one-electron Hamiltonian is then given by

$$H=\sum_{ii'}\sum_{mm'}\sum_{\sigma\sigma'}|im\sigma\rangle\langle i'm'\sigma'|\delta_{\sigma\sigma'}(\delta_{ii'}\delta_{mm'}\epsilon_i^{\sigma}+t_{i'm'}^{im}),$$

$$\epsilon_i^{\sigma}=\epsilon_i^0-\frac{\sigma}{2}I_iM_i. \tag{4}$$

The quantity ϵ_i^{σ} in Eq. (4) is the center of the $i\sigma$ band, while the $t_{i'm'}^{im}$ are the spin-independent interatomic hopping integrals, I_i is the effective exchange integral, and M_i is the local magnetic moment on site i. The self-consistent spin-independent energy levels ϵ_i^0 are obtained iteratively together with the self-consistent local magnetic moments M_i. The latter are defined in terms of the local occupations N_i^{σ} as $M_i=N_i^+-N_i^-$, while the values of ϵ_i^0 are chosen in order to satisfy a condition of local neutrality of all sites, i.e., the sum $N_i^++N_i^-$ must equal the value for the corresponding bulk metal. The local occupations N_i^{σ} are obtained by integration of the spin-polarized local densities of states of the Hamiltonian (4) up to the Fermi energy. The densities of states are calculated by means of the real-space recursion method[13] with eight levels of the continuous fraction and the Beer-Pettifor terminator.[14] The parameters $t_{i'm'}^{im}$ and I_i in Eq. (4) were set identical to Ref. 7: this choice reproduces the magnetic properties of bulk Fe and Cr metals as well as those of Cr films on Fe(001) obtained with an *ab initio* full-potential augmented-plane-wave method.

The magnetic moments are calculated self-consistently for all inequivalent atoms in the Cr overlayer, in the two mixed layers, and in ten iron layers below the interface. The magnetic moments of the rest substrate atoms are kept frozen to the Fe bulk value. In order to find the magnetic ground state for a given atomic configuration, total energies of the different self-consistent magnetic structures are evaluated and analyzed. The present scheme leads to numerical accuracy of the total energies better than 0.1 mRy per interface atom.

B. TB-LMTO-CPA method

The all-electron TB-LMTO-CPA method for substitutionally disordered layered systems[15–17] is based on the atomic-sphere approximation (ASA) and the exchange-correlation potential given in Ref. 18. The valence states were described using $l_{\max}=2$ and the scalar-relativistic approximation. In order to simplify the treatment of a simultaneous presence of chemical and magnetic disorder in the system, we assumed only one magnetic state for each atomic species (Fe, Cr) in a given layer. The coupled CPA conditions[16,17] were then solved, thus taking into account the inhomogeneity of the model system, Eq. (1). As a consequence, all interlayer and intralayer contributions to the LSDA-CPA total energy are fully included in the present approach. The spherically symmetric one-electron potentials within the individual atomic spheres were constructed not only from the spherical component of the electron charge (and spin) densities, but they included also the contribution to the Madelung term due to the dipole moments of the full charge densities.[19] Self-consistency of the one-electron potentials and the calculations of total energies were restricted to a finite region comprising 12 atomic layers (3 empty-sphere layers and 9 metallic layers) on top of an undisturbed semi-infinite Fe(001) substrate. The integrals over the occupied part of the valence bands were evaluated using 14 points on a semicircle contour in the complex energy plane. The irreducible part of the two-dimensional Brillouin zone was sampled by 45 special $\mathbf{k}_{\|}$ points. The accuracy of the Brillouin zone integrations with respect to local magnetic moments and the total-energy differences was checked for a few selected cases employing a greater number (120) of special $\mathbf{k}_{\|}$ points. The resulting total-energy differences are accurate within an error bar of 0.1 m Ry per interface atom.

IV. RESULTS AND DISCUSSION

A. 1-ML Cr/Fe(001) - $n=0$

1. Ordered alloys

For the 1-ML Cr overlayer with ordered interface alloys several different magnetic structures were found. An ex-

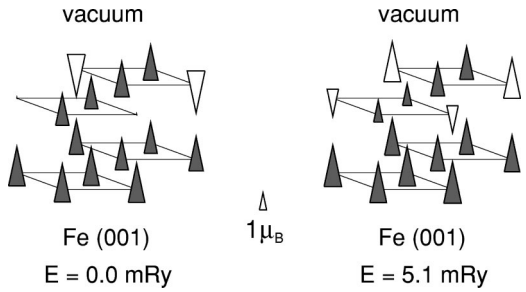

FIG. 2. The magnetic structure of the ground state (left) and the metastable state (right) found for $n=0$ and $x=0.5$ referring to an ordered alloy at the Cr/Fe interface. The empty and full triangles correspond to the Cr and Fe moments, respectively. The size of a triangle scales with the magnitude of the moment, while the triangle orientation defines the sign. The energy differences are given per interface atom.

ample of multiple solutions is shown in Fig. 2 for the case of $x=0.5$ (see Fig. 1 for the corresponding unit cell) for which two solutions were obtained. In both solutions, the Cr moments within one layer are coupled ferromagnetically, whereas they are coupled antiferromagnetically from layer to layer. The Cr surface moments for the ground state (left panel of Fig. 2) are coupled antiferromagnetically to the Fe substrate in contrast to the metastable state (right panel of Fig. 2) with ferromagnetic coupling. The Fe moments in all layers and for both solutions are coupled ferromagnetically to the bulk substrate.

Figure 3 shows the ground-state average magnetic moments for both species in the mixed layers: the top surface layer (S) and the first subsurface layer ($S-1$). The most remarkable feature of the plotted dependences is an abrupt change in the surface Cr moment around $x\approx 0.6$, which is accompanied by change of sign of this moment. The subsurface Cr moment exhibits a similar but less pronounced behavior, whereas the Fe moments in the mixed layers depend only weakly on x in the concentration range studied.

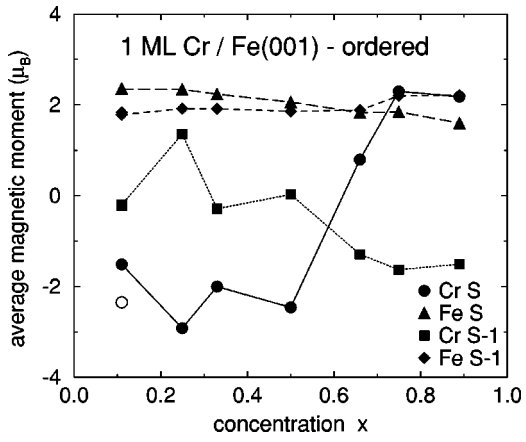

FIG. 3. Average ground-state Cr and Fe magnetic moments in the mixed layers as a function of x for $n=0$ referring to ordered alloys at the Cr/Fe interface. The open symbols correspond to a metastable solution that is nearly degenerate with the ground state.

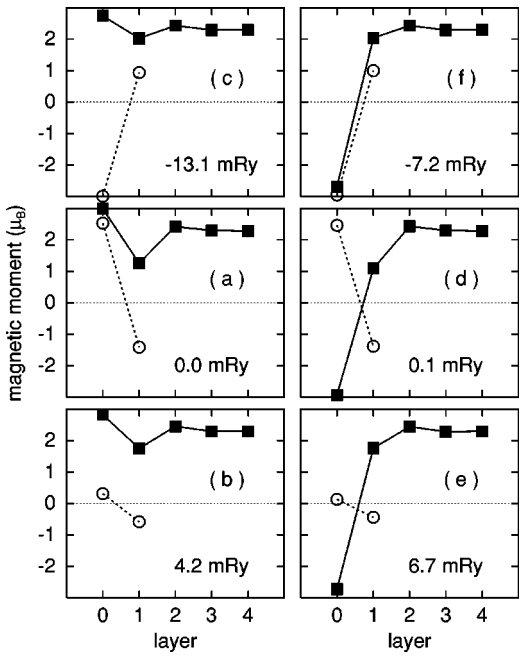

FIG. 4. The magnetic structures found for $n=0$ and $x=0.1$ referring to a random alloy at the Cr/Fe interface. The empty circles and the full squares correspond to the Cr and Fe moments, respectively. The energy differences are given per interface atom. The layer numbering starts at the top surface layer, denoted by 0.

2. Random alloys

Solving the LSDA-CPA self-consistency problem for 1-ML Cr systems with random interface alloys leads also to a number of different solutions that have to be classified according to the resulting spin structures and total energies. Figure 4 presents the magnetic profiles for all solutions found for $x=0.1$ together with their total energies relative to a particular given solution. The six solutions obtained correspond to combinations of the surface Cr moment having either a large positive, a large negative, or a small value, and of the surface Fe moment coupled ferromagnetically or antiferromagnetically to the bulk substrate. The values of the surface Fe moments are significantly enhanced as compared to the corresponding bulk value. The ground state [Fig. 4(c)] is featured by a large positive surface Cr moment, a smaller negative subsurface Cr moment, and positive Fe moments in all layers. The lowest metastable state [Fig. 4(f)] differs from the ground state only by a reversal of the surface Fe moment. It should be noted that the calculated magnetic ground state of the perfect 1-ML Cr film on Fe(001) ($x=0$) agrees with existing results for this system:[20–22] a large local Cr moment ($3\mu_B$) coupled antiferromagnetically to the substrate magnetization.

The concentration dependence of the ground-state local magnetic moments in the mixed layers is shown in Fig. 5. The individual moments exhibit behavior very similar to that in the ordered case (cf. Fig. 3): an abrupt change of both Cr moments around $x\approx 0.6$ and nearly constant positive Fe moments.

Figure 6 presents the total energy of all the different solutions found throughout the whole concentration range. We

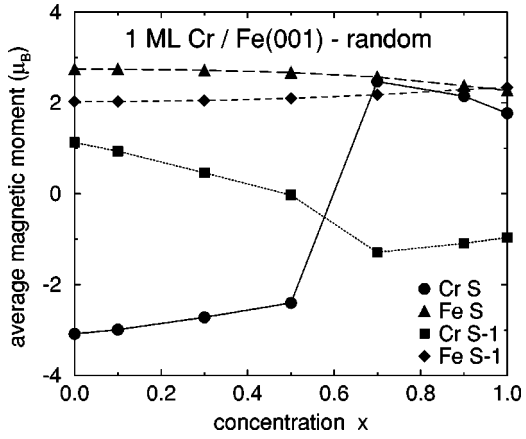

FIG. 5. Ground-state local Cr and Fe magnetic moments in the mixed layers as a function of x for $n=0$ referring to random alloys at the Cr/Fe interface.

took the solution in Fig. 4(a) (which exists from $x=0$ to $x=1$) as a reference system for the total energies. The abrupt change in Cr moment in Fig. 5 is now easily identified as a transition between two qualitatively different ground states [labels (a) and (c) in Figs. 4 and 6]. It should be noted that additional solutions to those in Fig. 4 were found for higher concentrations ($x \geqslant 0.5$). These solutions contain subsurface Fe moments coupled antiferromagetically to the Fe substrate. Inspection of their total energies (empty symbols in Fig. 6) proves that they represent metastable states lying relatively far above the ground state.

3. Comparison and discussion

The results for a 1-ML Cr film on a Fe(001) substrate both with ordered and disordered alloys show surprisingly similar concentration dependences, see Figs. 3 and 5: in both models the surface Cr moment changes its sign for concentration x slightly above $x=0.5$. This agreement indicates that both approaches describe essentially the same physical mechanism. As detailed accounts of the various spin solutions for our two models were given elsewhere,[7,23] let us concentrate here on a brief comparison and summary of the results.

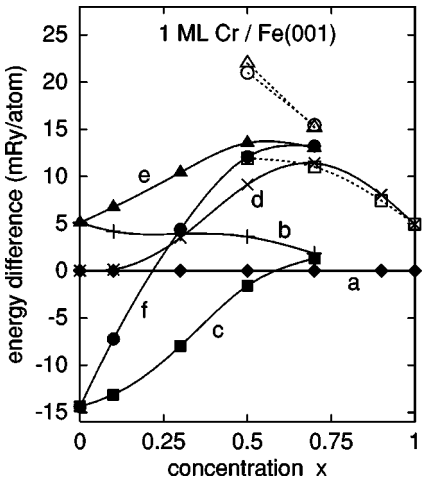

FIG. 6. Concentration dependence of energy differences (per interface atom) for various LSDA-CPA solutions for $n=0$ referring to random alloys at the Cr/Fe interface. The labels a–f correspond to those in Fig. 4. The empty symbols connected by dotted lines mark solutions with negative subsurface Fe moments.

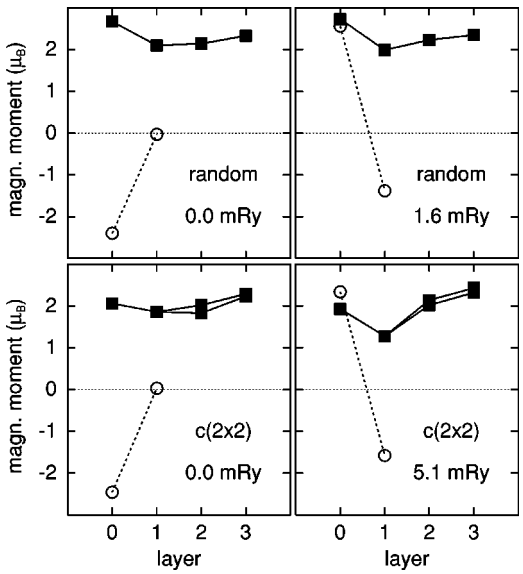

FIG. 7. Comparison of the magnetic structures for the ground states (left) and the lowest metastable states (right) obtained for $n=0$ and $x=0.5$ referring to a random alloy (top) and a $c(2\times2)$-ordered alloy (bottom) at the Cr/Fe interface. The empty circles and the full squares correspond to the Cr and Fe moments, respectively. The layer numbering starts at the top surface layer, denoted by 0.

In Fig. 7 the calculated spin structures of the ground state and of the lowest metastable state are compared for both models at $x=0.5$: it can be seen that the agreement is nearly perfect. The ground state of both models contains a large negative Cr moment in the top surface layer and a nearly negligible subsurface Cr moment. The metastable state con-

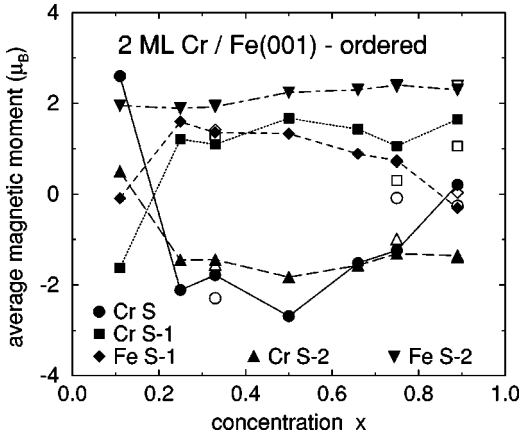

FIG. 8. Average ground-state Cr and Fe magnetic moments in the top surface layer (S) and the first ($S-1$) and second ($S-2$) subsurface layers as a function of x for $n=1$ referring to ordered alloys at the Cr/Fe interface. The open symbols correspond to metastable solutions that are nearly degenerate with the ground state.

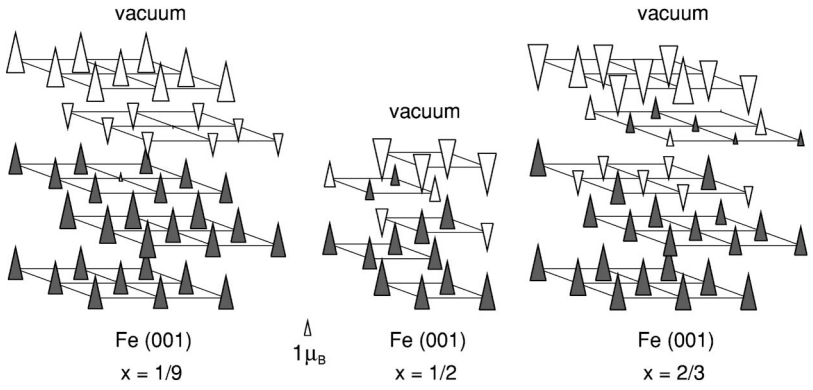

FIG. 9. The ground-state magnetic structures found for $n=1$ and three values of x referring to ordered alloys at the Cr/Fe interface. The empty and full triangles correspond to the Cr and Fe moments, respectively.

tains a large positive Cr surface moment and a smaller (but well-developed) negative subsurface Cr moment. The only quantitative difference between the two models refers to the magnitude of the Fe moments: the SE-TB approach yields smaller iron moments at the surface, while LSDA-CPA iron moments are clearly enhanced as compared to the bulk Fe value. This behavior is in full analogy to *ab initio* results for systems without interdiffusion.[16,20,24]

The basic species-resolved magnetic exchange interactions in the Cr/Fe alloy systems can be inferred, e.g., from the ground-state spin structure for $x=0.1$ [Fig. 4(c)]: the nearest-neighbors (NN) Cr-Cr moments prefer an antiferromagnetic coupling, the NN Fe-Fe moments tend to align ferromagnetically, and the NN Cr-Fe moments are coupled antiferromagnetically. Quite clearly, these tendencies can be fully satisfied only for chemically perfect systems ($x=0$ and $x=1$). The interdiffused systems become inevitably frustrated, which leads to a number of competing spin structures. The magnetic frustrations are responsible not only for the observed reversal of the surface Cr moment at $x\approx 0.6$ but also for the reduction of the sizes of particular local moments,[7,23] as illustrated, e.g., by the subsurface Cr moment in the ground states for $x=0.5$, see Fig. 7.

B. 2-ML Cr/Fe(001) - $n=1$

1. Ordered alloys

Multiple solutions were found also for the case of a 2-ML Cr coverage. The average ground-state local moments are summarized in Fig. 8 as functions of x. The behavior of the average Cr moment in the top surface layer (S) is quite unexpected. For small values of x, this moment is large and positive, it changes sign at $x\approx 0.2$, remains negative up to $x\approx 0.75$, and finally vanishes for yet higher values of x.

In addition to the averaged moments the individual spin structures are shown in Fig. 9 for three values of x. It can be seen that the site- and species-resolved local moments for $x \leqslant 0.5$ do not deviate significantly from the corresponding layer averages shown in Fig. 8. For higher concentrations, the top surface Cr moments exhibit large fluctuations around the average, and the surface layer consists of large moments of both signs (cf. Fig. 9 for $x=0.67$). As observed in Fig. 8, this kind of in-plane antiferromagnetism then reduces the average surface Cr magnetization for high concentrations. The values of the Fe moments are positive in the whole concentration range studied; the only exceptions are the nearly vanishing Fe moments in the first subsurface layer at $x=0.11$ and $x=0.89$. The Fe moments in the second and next subsurface layers are nearly constant with a value close to that of bulk bcc iron.

2. Random alloys

For 2-ML Cr and a randomly interdiffused Cr/Fe interface, the number of different LSDA-CPA solutions found for a given concentration was at least 8 (and exceeded 12 for $x \geqslant 0.7$). However, the ground-state configurations result from a competition among three qualitatively different spin structures listed in Table I. The ground-state structure for small x (label a in Table I for $x=0.1$) is derived from that of a perfect Cr bilayer on Fe(001):[20] a large surface Cr moment coupled ferromagnetically to the Fe substrate and a smaller Cr subsurface moment coupled antiferromagnetically. For intermediate and high concentrations of interdiffusion the sign of the surface Cr moment is changed (labels b and c in Table I for $x=0.5$ and 0.9, respectively). The difference between the ground states at $x=0.5$ and $x=0.9$ is due to the first subsurface Fe moment, being slightly negative for $x \geqslant 0.9$.

TABLE I. The ground-state local magnetic moments (in μ_B) for 2-ML Cr films on a Fe(001) substrate with random alloys at the Cr/Fe interface for three values of x. Only the moments in the top surface layer (S) and in the first three subsurface layers ($S-1$, $S-2$, $S-3$) are given.

x	Label	Cr(S)	Cr($S-1$)	Fe($S-1$)	Cr($S-2$)	Fe($S-2$)	Fe($S-3$)
0.1	a	2.65	−1.34	1.70	0.27	2.19	2.32
0.5	b	−2.81	1.14	1.83	−0.99	2.29	2.17
0.9	c	−2.92	1.11	−0.39	−0.85	2.43	2.07

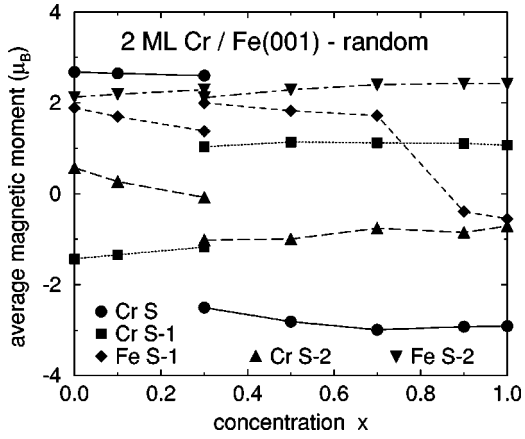

FIG. 10. Ground-state local Cr and Fe magnetic moments in the top surface layer (S) and the first ($S-1$) and second ($S-2$) subsurface layers as a function of x for $n=1$ referring to random alloys at the Cr/Fe interface.

As shown in Fig. 10, the concentration dependence of the individual moments is relatively weak: the only abrupt changes occur at $x=0.3$ for all moments and at $x\approx 0.8$ for the first subsurface Fe moment. The total energies for the most stable solutions are presented in Fig. 11. It can be seen that the energy separations for small concentrations ($x \leqslant 0.2$) are quite pronounced in contrast to higher values of x where the three competing solutions (labeled by a, b, and c) become nearly degenerate.

3. Comparison and discussion

A comparison of concentration dependence of the ground state of 2-ML Cr films with ordered and random Cr/Fe interfaces (Figs. 8 and 10) reveals good overall agreement between both cases. First, a transition from the ground state of the perfect Cr bilayer ($x=0$) with a positive surface Cr moment to a different ground state with a negative surface Cr moment is observed. This transition occurs for relatively small values of x, namely, at $x\approx 0.2$ and $x=0.3$ for the ordered and disordered cases, respectively. Second, another transition in the ground-state configuration is observed for higher values of x, namely, at $x\approx 0.7$ and $x\approx 0.8$ for the ordered and disordered cases, respectively. In both cases, this transition is accompanied by a sign change and a reduction in size of the first subsurface Fe moment.

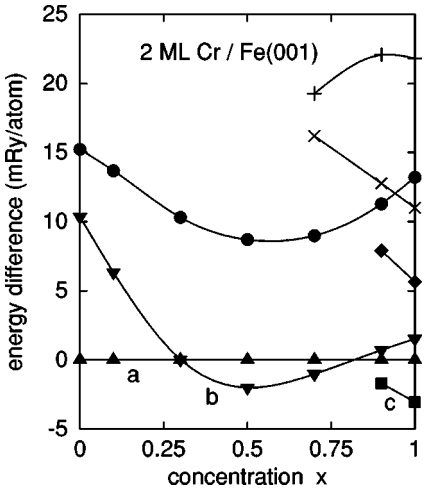

FIG. 11. Concentration dependence of the energy differences (per interface atom) for various LSDA-CPA solutions for $n=1$ referring to random alloys at the Cr/Fe interface. The labels a, b, and c correspond to Table I. Higher metastable solutions are omitted in the plot.

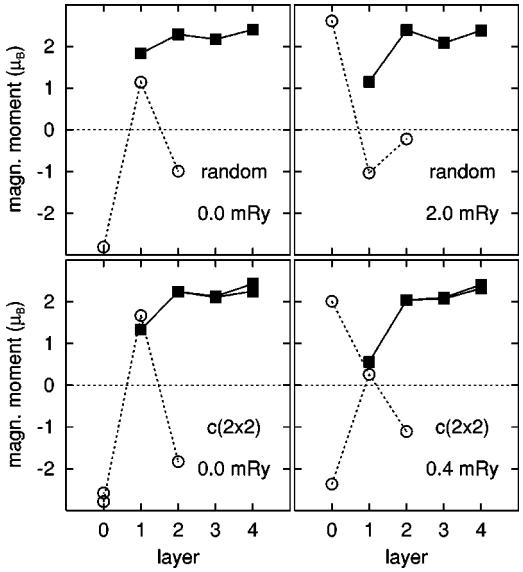

FIG. 12. Comparison of the magnetic structures for the ground state (left) and the lowest metastable state (right) obtained for $n=1$ and $x=0.5$ referring to a random alloy (top) and a $c(2\times 2)$-ordered alloy (bottom) at the Cr/Fe interface. The empty circles and the full squares correspond to the Cr and Fe moments, respectively. The layer numbering starts at the top surface layer, denoted by 0.

However, there are also qualitative discrepancies between the two cases. One of them is the value of the first subsurface Fe moment for small concentrations: this moment is negligible for ordered alloys at $x=0.11$ (Fig. 8), whereas it is quite large and positive in the random case for $x\rightarrow 0$ (Fig. 10). Another difference concerns the average surface Cr moment for higher concentrations ($x\geqslant 0.5$): it remains large and negative in the random case, whereas its magnitude decreases (essentially down to zero at $x=0.89$) in the ordered case.

The origin of the last discrepancy can be understood from Fig. 12, which shows the two lowest energy solutions obtained for both cases at $x=0.5$. While a reasonable agreement is seen for the ground states, the metastable solutions differ substantially: the pure surface Cr layer exhibits an in-plane antiferromagnetism in the case of ordered alloys, which is qualitatively different from the CPA solution assuming a fixed sign of the local moment for each species in a given layer. The displayed metastable state at $x=0.5$ in the ordered case (Fig. 12) becomes the ground state for higher concentrations (cf. Fig. 9 for $x=0.67$) and the in-plane antiferromagnetism reduces the average surface Cr magnetization.

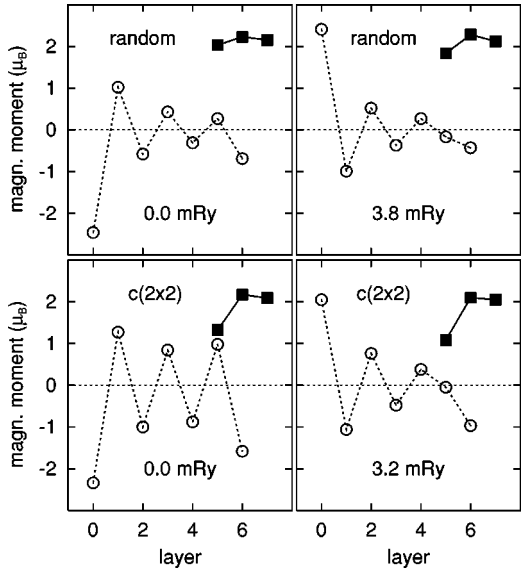

FIG. 13. Comparison of the magnetic structures for the ground state (left) and the lowest metastable state (right) obtained for $n=5$ and $x=0.5$ referring to a random alloy (top) and a $c(2\times2)$-ordered alloy (bottom) at the Cr/Fe interface. The empty circles and the full squares correspond to the Cr and Fe moments, respectively. The layer numbering starts at the top surface layer, denoted by 0.

The transition in the ground-state configuration at small values of x, found in both cases and accompanied by a change of sign of the top surface Cr moment (π phase shift), can explain some of the discrepancies between existing theories and experiments. Let us emphasize that an occurrence of the π phase shift due to the Cr/Fe interface intermixing can be easily understood (and could be anticipated) on the basis of the exchange interactions between the NN pairs in the frustrated Cr-Fe system (see Sec. IV A 3 and Ref. 7). However, it is the relatively small degree of the intermixing (corresponding to $x\approx0.2$ or $x=0.3$ in our models) that makes this mechanism highly relevant for currently prepared metallic multilayers.[5]

C. 6-ML Cr/Fe(001) - $n=5$

Finally, let us briefly summarize the results obtained for a 6-ML Cr coverage. Throughout the whole concentration interval, only two qualitatively different ground-state configurations were found, irrespective of the chemical order in the interdiffused layers. These two competing spin structures are shown for $x=0.5$ in Fig. 13. They correspond to an antiferromagnetic coupling between the neighboring pure Cr layers with an enhanced moment in the top surface Cr layer. The only qualitative difference between these two spin structures is the different sign of the surface Cr moment.

For the system with ordered interface alloys and for all concentrations studied, the above two solutions were the only ones found by the SE-TB scheme. The concentration dependence of the ground-state average local moments, depicted in Fig. 14, proves that a transition (π phase shift) between the two different states takes place at $x\approx0.2$ similarly to the case $n=1$ (cf. Fig. 8).

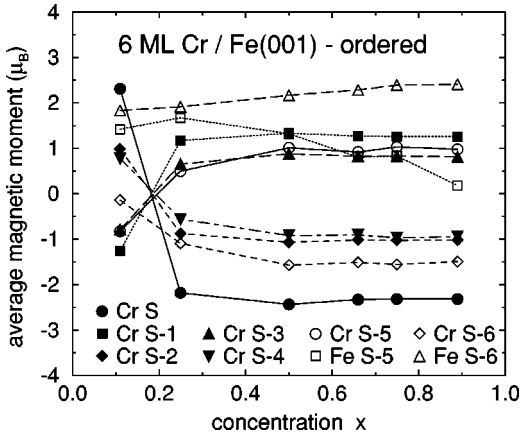

FIG. 14. Average ground-state Cr and Fe magnetic moments in the top surface layer (S) and the first five ($S-1$ to $S-5$) subsurface layers as a function of x for $n=5$ referring to ordered alloys at the Cr/Fe interface. The full symbols refer to the pure Cr layers; the open ones refer to the two mixed Cr-Fe layers.

The number of different LSDA-CPA solutions for the films with the disordered interface was substantially higher than 2 for each concentration (e.g., 11 for $x=0.7$). The higher lying metastable solutions were characterized either by a different magnetic order at the interface, or by magnetic defects in the pure Cr film (nearly vanishing Cr moments, ferromagnetically coupled neighboring Cr layers). However, as is documented by the behavior of the local moments in Fig. 15, as well as by the concentration dependence of the total-energy differences in Fig. 16, the ground-state configuration undergoes a very similar transition like that in the ordered-alloy case (cf. Fig. 14). The π phase shift occurs now at $x=0.25$, i.e., at a smaller concentration than found for the 2-ML Cr film (cf. Fig. 10). Similar to the cases $n=0$ and $n=1$, the origin of the π phase shift can be explained as a consequence of magnetic frustrations due to intermixing at the Cr/Fe interface.

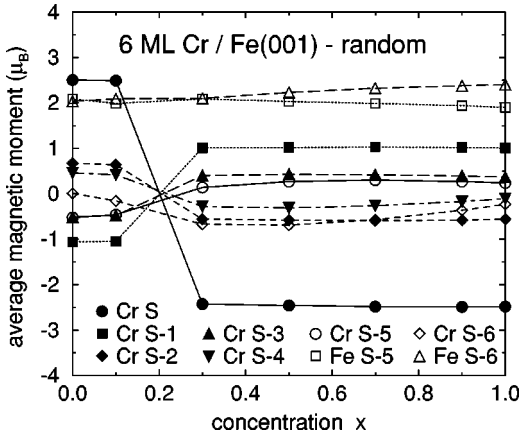

FIG. 15. Ground-state local Cr and Fe magnetic moments in the top surface layer (S) and the first five ($S-1$ to $S-5$) subsurface layers as a function of x for $n=5$ referring to random alloys at the Cr/Fe interface. The full symbols refer to the pure Cr layers; the open ones refer to the two mixed Cr-Fe layers.

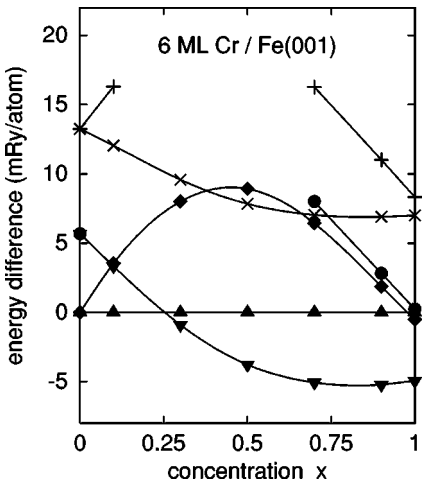

FIG. 16. Concentration dependence of energy differences (per interface atom) for various LSDA-CPA solutions for $n=5$ referring to random alloys at the Cr/Fe interface. Higher metastable solutions are omitted in the plot.

Let us finally make a quantitative comparison of the spin structures in the two competing states and for the two chemical orders considered. As can be seen in Fig. 13 for $x=0.5$, the magnitudes of the Cr magnetic moments calculated by the SE-TB method are systematically greater than the LSDA-CPA results, especially for layers well below the surface. This discrepancy can be ascribed to the fact that standard LSDA calculations have a tendency to underestimate the local moments in bulk bcc chromium,[12,25] whereas the SE-TB scheme uses the experimental bulk Cr moment as an input to fix the parameters of the Hamiltonian (4). However, the LSDA moments at the Cr surface are influenced mainly by the surface magnetic enhancement and can be considered reliable. This is probably one of the reasons for a very good quantitative agreement between the SE-TB and TB-LMTO-CPA values of the Cr moments in the top surface and first subsurface layers (Fig. 13).

V. CONCLUSIONS

We have investigated the electronic structure, magnetic moments, and exchange coupling in thin Cr films on a Fe(001) substrate in the presence of interdiffusion at the interface. The interdiffusion was taken into account in terms of two-dimensional ordered and disordered alloys located in the two neighboring layers forming the interface. The electronic structure was calculated by a semiempirical tight-binding scheme for the ordered interfaces and by the first-principle TB-LMTO-CPA method for the random interfaces.

The results of both approaches exhibit a reasonable semiquantitative agreement with each other which, in turn, proves that the basic mechanism driving the exchange coupling of the imperfect Cr overlayers to the iron substrate is not very sensitive to the details of the applied model. The most important fact is undoubtedly the π phase shift in the sign of the surface Cr moment that is due to intermixing and magnetic frustrations. This π phase shift was found in both theoretical models and—for Cr coverages greater than 1 ML—at relatively small degrees of intermixing (corresponding to an interchange of 20–30 % of atoms in the two neighboring layers). The same features were observed in recent experiments on Fe/Cr/Fe(001) trilayers and ascribed to intermixing at one of the interfaces.[5]

However, there are still points to be clarified in the future. On the theoretical side, some differences were found in the two sets of results, which might be explained either by different calculational procedures (the size of Cr moments inside thicker Cr films) or by different models adopted (the in-plane antiferromagnetism in pure Cr layers). As concerns the relation of theory to experiment, systems with intermixing in a single layer, described by the model $Cr_n/Cr_xFe_{1-x}/Fe(001)$, remain yet to be understood: too big a difference was found between the theoretical[7] and experimental[5] determination of the transition concentration for the π phase shift in this case.

ACKNOWLEDGMENTS

This work was supported by the Grant Agency of the Czech Republic (No. 202/97/0598), the Czech Ministry of Education, Youth, and Sports (No. OC P3.40), the Austrian Ministry of Science (No. GZ 45.442), the Project ''Scientific and Technological Cooperation between Germany and the Czech Republic'' (No. TSR-013-98), the TMR Network ''Interface Magnetism'' (No. EMRX-CT96-0089), and the RTN Network ''Computational Magnetoelectronics'' (No. RTN1-1999-00145). Part of the calculations were performed on the Origin 2000 ''Seven'' of the University Louis Pasteur of Strasbourg.

[1] P. Grünberg, R. Schreiber, Y. Pang, M. B. Brodsky, and H. Sowers, Phys. Rev. Lett. **57**, 2442 (1986).
[2] S. S. P. Parkin, N. More, and K. P. Roche, Phys. Rev. Lett. **64**, 2304 (1990).
[3] S. Mirbt, A. M. N. Niklasson, B. Johansson, and H. L. Skriver, Phys. Rev. B **54**, 6382 (1996).
[4] J. Unguris, R. J. Celotta, and D. T. Pierce, Phys. Rev. Lett. **69**, 1125 (1992).
[5] B. Heinrich, J. F. Cochran, T. Monchesky, and R. Urban, Phys. Rev. B **59**, 14 520 (1999).
[6] D. Stoeffler and F. Gautier, Prog. Theor. Phys. Suppl. **101**, 139 (1990).
[7] M. Freyss, D. Stoeffler, and H. Dreyssé, Phys. Rev. B **56**, 6047 (1997).
[8] A. Davies, J. A. Stroscio, D. T. Pierce, and R. J. Celotta, Phys. Rev. Lett. **76**, 4175 (1996).
[9] D. Venus and B. Heinrich, Phys. Rev. B **53**, R1733 (1996).
[10] R. Pfandzelter, T. Igel, and H. Winter, Phys. Rev. B **54**, 4496 (1996).
[11] R. Coehoorn, J. Magn. Magn. Mater. **151**, 341 (1995).

[12] A. B. Klautau, S. B. Legoas, R. B. Muniz, and S. Frota-Pessôa, Phys. Rev. B **60**, 3421 (1999).
[13] R. Haydock, in *Solid State Physics*, edited by H. Ehrenreich, F. Seitz, and D. Turnbull (Academic, New York, 1980), Vol. 35, p. 215.
[14] N. Beer and D.G. Pettifor, in *The Electronic Structure of Complex Systems*, edited by P. Phariseau and W. M. Temmerman (Plenum, New York, 1984), p. 769.
[15] J. Kudrnovský, I. Turek, V. Drchal, P. Weinberger, N. E. Christensen, and S. K. Bose, Phys. Rev. B **46**, 4222 (1992).
[16] I. Turek, V. Drchal, J. Kudrnovský, M. Šob, and P. Weinberger, *Electronic Structure of Disordered Alloys, Surfaces and Interfaces* (Kluwer, Boston, 1997).
[17] I. Turek, J. Kudrnovský, and V. Drchal, in *Electronic Structure and Physical Properties of Solids*, edited by H. Dreyssé, Lecture Notes in Physics Vol. 535 (Springer, Berlin, 2000), p. 349.
[18] S. H. Vosko, L. Wilk, and M. Nusair, Can. J. Phys. **58**, 1200 (1980).
[19] H. L. Skriver and N. M. Rosengaard, Phys. Rev. B **43**, 9538 (1991).
[20] S. Mirbt, O. Eriksson, B. Johansson, and H. L. Skriver, Phys. Rev. B **52**, 15 070 (1995).
[21] S. Handschuh and S. Blügel, Solid State Commun. **105**, 633 (1998).
[22] T. Asada, G. Bihlmayer, S. Handschuh, S. Heinze, Ph. Kurz, and S. Blügel, J. Phys.: Condens. Matter **11**, 9347 (1999).
[23] I. Turek, P. Weinberger, M. Freyss, D. Stoeffler, and H. Dreyssé, Philos. Mag. B **78**, 637 (1998).
[24] A. J. Freeman and R. Wu, J. Magn. Magn. Mater. **100**, 497 (1991).
[25] E. G. Moroni and T. Jarlborg, Phys. Rev. B **47**, 3255 (1993).